Princeton Plasma Physics Laboratory

PPPL- 4826

PPPL- 4826

PTRANSP Tests of TGLF and predictions for ITER

R.V. Budny, Xingqiu Yuan, S. Jardin, G. Hammett, G. Staebler, J. Kinsey,
Members of the ITPA Transport and Confinement Topical Group,
and JET EFDA Contributors

October, 2012

Prepared for the U.S. Department of Energy under Contract DE-AC02-09CH11466.

Princeton Plasma Physics Laboratory
Report Disclaimers

Full Legal Disclaimer

Trademark Disclaimer

PPPL Report Availability

Princeton Plasma Physics Laboratory:

http://www.pppl.gov/techreports.cfm

Office of Scientific and Technical Information (OSTI):

http://www.osti.gov/bridge

Related Links:

U.S. Department of Energy

Office of Scientific and Technical Information

Fusion Links

PTRANSP tests of TGLF and predictions for ITER

R.V. Budny[1], Xingqiu Yuan[1], S. Jardin[1], G. Hammett[1], G. Staebler[2], J. Kinsey[2],
members of the ITPA Transport and Confinement Topical Group, and JET EFDA Contributors*

[1]PPPL, P.O. Box 451, Princeton, NJ 08543, USA;
[2]General Atomics, San Diego, CA, USA;

e-mail contact of the main author: budny@princeton.edu

Abstract
A new numerical solver for stiff transport predictions has been developed and implemented in the PTRANSP predictive transport code. The TGLF and GLF23 predictive codes have been incorporated in the solver, verified by comparisons with predictions from the XPTOR code, and validated by comparing predicted and measured profiles. Predictions for ITER baseline plasmas are presented.

1. Introduction - One of the physics goals for ITER is to achieve high fusion power $P_{\rm DT}$ at high gain $Q_{\rm DT}$. This goal is important for studying the physics of reactor-relevant burning plasmas. Simulations of plasma performance in ITER can help achieve this goal by aiding in the design of systems such as diagnostics and in planning ITER plasma regimes. Simulations can indicate areas where further research in theory and experiments is needed. Integrated modeling is necessary to have credible simulations since plasma profiles and applied heating, torque, and current drive are strongly coupled.

Self-consistent predictions for ITER need to predict profiles of temperatures, densities, rotation, plasma current, etc. The predictions need to describe the core region since the alpha heating is expected to be especially peaked in the core. The predictions need to include the pedestal and edge regions since these affect the core.

The PTRANSP code [1–6] is an upgrade of the TRANSP analysis code with added predictive features. It can generate self-consistent, time-dependent integrated predictions. Time dependent predictions are necessary to include evolving processes such as plasma formation, termination, and transients such as magnetic field diffusion, sawtooth effects, and accumulation of ash from the DT reactions. The PTRANSP predictions are self-consistent in that the heating, current-drive, torques and equilibria are calculated using predicted plasma profiles, and vice versa. These are included in the local flux-surface averaged energy, momentum, and magnetic field evolutions.

Physics-based models are needed to predict plasma profiles. One model, GLF23 [7] has achieved approximate agreement predicting measured temperatures and toroidal rotation v_ϕ. Examples of predictions are in Ref. [8]. There are important physics effects not included in GLF23. One example is general-shaped flux geometry. An improved Trapped Gyro-Landau Fluid model TGLF [9, 10] contains physics not included in GLF23 such as realistic shaped finite aspect ratio (Miller) flux geometry, collisionality, and a larger set of basis functions for fitting the ITG, TEM, ETG, and electromagnetic kinetic ballooning mode turbulence simulated with a large database of non-linear runs using the GYRO code [11]. TGLF achieves more accurate predictions of temperatures measured in DIII-D and JET L-mode, H-mode and hybrid discharges than does GLF23 [12, 13].

This paper describes a major upgrade to PTRANSP using a new robust solver for stiff transport models. The GACODE repository versions of TGLF and GLF23 models have been incorporated so far. The implementation of TGLF is verified by comparing with results derived using the XPTOR code, and is tested using L-mode, H-mode, and Hybrid plasmas from JET, DIII-D, and TFTR. Predictions for ITER plasmas are given and compared with predictions using GLF23.

*See the Appendix of F. Romanelli, *et al.,* Proceedings of the 24th IAEA Fusion Energy Conference 2012, San Diego, US

2. PT-SOLVER - The new solver is modular, parallel, and multi-regional. The solver does not depend on PTRANSP internals and is being made available through the NTCC website [14]. PT-SOLVER integrates the highly nonlinear time-dependent equations for ion and electron temperatures, densities, and toroidal angular momentum with implicit Newton iteration methods. The user controls the choice of transport models attached to the solver, with a range of neoclassical and/or turbulent, or semi-empirical or data driven choices available. Besides TGLF and GLF23 the neoclassical models NEO, NCLASS, and Chang-Hinton are included.

A multi-level parallelization paradigm has been implemented, with which the number of CPUs is not limited by the number of zones in flux-surface. The parallelization is over flux-surfaces and the k_y spectrum domain. This new specific design pattern makes it possible to perform time-dependent predictions together with very computationally intensive turbulent models such as TGLF. The multi-level parallelization is implemented by recursively splitting the MPI communicators into daughter communicators. The final layouts of the communicator form a tree topology, and the number of CPUs in each communicator can be dynamically adapted depending on the CPU loading (not available in PT-SOLVER presently). This allows the code to run on a flexible number of CPUs.

When using stiff turbulent models such as TGLF, the standard implicit time integration algorithm such as Crank-Nicolson or backward Euler can lead to large non-physical oscillations. In PT-SOLVER, two methods are used to prevent this. One, from [15] uses a linear implicit approximation to the turbulent transport coefficients when applying implicit newton iterations. The second, from [16] uses uses a power law scheme which modifies the prandtl number by adding an artificial numerical viscosity.

The data are communicated between PTRANSP and PT-SOLVER via "plasma-state software" [17] . which is used to store axisymmetric MHD equilibrium, plasma and source profiles for both 1D and 2D data, and associated scalar variables. The Miller approximation to the general flux geometry is passed to TGLF. The interface provides easy data access (allowing, for instance, rezone and interpolation function etc). The data used in the plasma-state is component based fortran 90 type. Presently the PT-SOLVER does not include time-rate-of-change data.

The inputs to PT-SOLVER are provided by a "plasma state" netcdf file summarizing plasma conditions at a time slice. The file can be written from a TRANSP or PTRANSP run. TGLF allows up to five ion species. A variable number of species can be used in PT-SOLVER. The inputs provided by the plasma state include profiles of the thermal plasma species (ex, H, D, T) fast ion species stored in three different categories as beam, alpha, and ICRH minorities, and impurities (ex, C, Ar, He, and ash) stored with averaged charge states. For TRANSP analysis of shots with measured impurity ion temperature the plasma state file provides T_i for the bulk ion species. Using the plasma species profiles from plasma state, PT-SOLVER combines each category together with appropriate atomic mass and charge state profiles and feeds them into TGLF.

The unstable modes included in the predictions can be varied. Two modes are included in the fitting of TGLF to GYRO. For the results presented here two are used. Runs with up to four have been compared. The number of k_y modes used is 21 (9 with $k_y \leq 1$, and 12 with $k_y > 1$). PT-SOLVER can output the frequency and growth rate and the electron and ion heat and particle fluxes at each unstable mode, k_y, and radial zone. Results here predict either T_e and T_i, or T_e, T_i, n_e, and n_i.

TGLF has been tested with up to up to 128 parallel CPU's achieving very good scalability. Typical runs with PTRANSP using TGLF (such as 5 sec for the DIII-D ITER demo baseline 148773 shown below) take about two and half days using 64 cores in the PPPL Dawson cluster. The standalone PT-SOLVER TGLF runs with 40 zones on 32 cores take about 3 minutes per time step.

3. Verification - The implementation of TGLF in PT-SOLVER is verified by comparing with predictions by XPTOR (the standard code for GLF23 and TGLF predictions). Both codes start with profiles at a time slice and evolve them to stationary solutions. The plasma state files provide inputs with two inter-spliced radial axes, one used for zone-centered quantities, and one used for zone-boundary quantities for the purpose of improving the accuracy of local conservation laws. XPTOR was altered to be able to input both. This results in more accurate agreement between both codes.

A crucial check is comparison of the heat and particle flux profiles predicted prior to evolving solutions. Such comparisons for a discharge are shown in Figure 1. The PT-SOLVER and XPTOR predictions are in approximate agreement. Different formulations for the differencing schemes (first order in XPTOR and second order in PT-SOLVER) lead to small differences in the predictions. Predictions for the heat fluxes after iterating to steady-state are shown in Figure 2.

The numerical convergence in PT-SOLVER is checked several ways. One by comparing the fluxes computed by TGLF with those computed by volume-integrating the sources. Profiles computed both ways converge with iteration to a near match. Another check is by examining convergence of the time-evolution of the profiles. These obtain steady-state after sufficient iteration. Another check of the treatment of multiple ions is comparison of the local charge density. The profiles of the net charge density are near zero.

4. Validation - The TGLF model is tested by comparing with experimental data. Several issues complicate comparisons. TGLF transport is negligible from the magnetic axis out to a flux surface with x defined as the square-root of the normalized toroidal flux of about 0.2-0.3. If only TGLF is assumed in this inner region too high central temperatures are predicted. Possible turbulence spreading and MHD effects are not predicted in TGLF. Sawteeth and other, sometimes difficult to observe MHD can effect plasma profiles in the core, and thus complicate comparisons with data.

Models for neoclassical transport can be added to the TGLF-driven transport for comparisons with experimental data. For the TGLF results shown here the electron and thermal ion energy and electron particle transport near the axis are increased by: $\chi_e/\chi_{CH} = 5$, $\chi_i/\chi_{CH} = 2$, and $D_e/\chi_{CH} = 1$, with χ_{CH} the Chang-Hinton neoclassical thermal ion conduction profile. Also sawteeth effects can have large effects on core profiles. TRANSP has a generalized Kadomtsev model for sawteeth mixing, but sawteeth effects are ignored here.

Accurate measurements of plasma profiles are needed for accurate computation of profiles of heat, particle, and momentum flows. Besides T_e, T_i, and v_ϕ, profiles of $Z_{\rm eff}$ and radiation and charge-exchange losses are needed. Anomalous transport of fast ions also can complicate comparison with measurements. For instance the deposition profiles of heat from beam, fusion, and ICRF-accelerated ions is needed by TGLF. Often the TRANSP analysis providing these profiles assumes classical slowing down and pitch-angle scattering.

Plasma properties near the scrape off region are difficult to predict and to measure. Typical assumptions of gyro-kinetic models are not satisfied in regions with steep gradients, which often occur near the edge. Also measurements of profiles such as ion temperature, rotation, and $Z_{\rm eff}$ are challenging in the edge. Comprehensive predictions for ITER require predictions in both the core and edge regions. Temperatures and the D and T densities in the core are needed for prediction the fusion energy production. Conditions in the pedestal region are also important since plasma profiles are expected to be stiff with limited gradients. Thus large pedestal temperatures are correlated with large core temperatures.

The PT-SOLVER module has been tested using data from TFTR, DIII-D, and JET. The plasma regimes include L-mode, H-mode, and Hybrid. Comparisons are done using various numbers of plasma species (2-4 so far), and either including or not turbulence quenching by flow shear.

Figure 3 shows results for a JET D H-mode plasma with the high density and plasma current (4.5MA) [18]. The toroidal magnetic field is 3.6T and the heating is 23MW of beam injection and 3MW of ICRH. The TGLF electron heat flux is negligible inside x=0.35. The XPTOR and PT-SOLVER TGLF predictions and T_e measurements (from ECE) are in approximate agreement between x=0.35 and 0.8 (the boundary for the predictions). The GLF23 predictions are lower. The TGLF ion heat flux is negligible inside x=0.25. The predictions are higher than the T_i measurements, even between x=0.25 and 0.8. This and similar high I_p plasmas under-perform in that the energy confinement times are less than expected. For instance their H_{98y2} tend to decrease with I_p. This might be correlated with the over-prediction of TGLF. Comparisons have also been performed for the JET DT H-mode plasma with the highest $Q_{\rm DT}$ (0.2) [19].

Figure 4 shows results for a JET D L-mode with I_p=2.5MA, B_0=2.6T, and 3MW of beam injection. The TGLF boundary is set at x = 0.85. The TGLF heat flows are negligible for x $\leq$ 0.2. The T_e prediction is in approximate agreement with measurements (from ECE), but the T_i prediction is high. The increases of T_e and T_i within x = 0.2 indicate that the assumed transport is too small. Typically TGLF and GYRO predict too little turbulent transport near the edge (x greater than $\simeq$ 0.7) in L-mode plasmas [20].

PT-SOLVER-TGLF predictions were performed also including the electron and effective ion densities keeping Z_{eff} fixed. The source rate for the electron density is computed from the beam ionization rate and estimates of the recycling, fueling, and gas puffing rates derived from the H_α and gas puffing rates. The measured and predicted densities are shown in figures 4-c) and 4-d). Typically TGLF predicts densities more peaked than measured.

Figure 5 shows results for a JET Hybrid [21] with I_p ramped down to 1.8MA, B_0=2.3T, and heated by 18MW beam injection, achieving H_{98y2}=1.3. Both T_e and T_i predictions are high. Predictions including density evolution (shown) achieve a slightly better prediction of T_i.

Figure 6 shows results for a DIII-D experiment investigating the stability and confinement in ITER baseline scenario discharges. This plasma had I_p=1.2MA and B_0=1.6T. The TGLF ion heat flux is negligible inside x=0.2. The predicted T_e is higher than the fit through the measurements. The predicted T_i is close to the fit through the measurements. Predictions including electron and ion density (not shown) are higher.

5. Predictions - ITER H-mode plasma predictions using the GLF23 and TGLF are compared. Plasma state inputs are taken from a PTRANSP time-evolved prediction [6] using GLF23 in the old PTRANSP solver for the temperature profiles. The toroidal field is held at 5.3T and the plasma current ramps up to a flat top value of 15MA. The electron density profile is assumed to be nearly flat out to the pedestal region and is ramped up to a flat top Greenwald fraction of 0.85. The H-mode phase starts during the phase with the maximum applied power planned: 33MW beam injection, 20MW ICRF, and 20MW ECRF. After the alpha heating builds up the applied heating is reduced to 33MW beam injection and 17MW ICRF. The β_n is 1.92. The pedestal temperatures are assumed to be 4.4keV and are used as boundary conditions. The pressure in the pedestal, with $\beta_{n,ped}$=0.7 is close to the maximum expected to be MHD stable.

The toroidal rotation rate predicted from the PTRANSP-computed beam torque assuming a ratio of transport coefficients $\chi_\phi/\chi_{i,glf23}$=0.5 is v_ϕ=12 kRad/s. The strength of the E×B flow shear, assumed to be 1.0, is predicted by PTRANSP with GLF23 to have a modest effect on T_e and T_i. That prediction achieved $Q_{\rm DT}$=6 with 73MW external heating and 9 during the phase when the heating is lowered to 50MW.

The plasma state file taken at 245 sec, between sawteeth and with P_{ext}=50MW is used for inputs for PT-SOLVER. Figure 7 shows comparisons of predictions. The TGLF transport is negligible for x $\leq$ 0.15. As in the validation cases discussed above, the transport near the axis is assumed to be: $\chi_e/\chi_{CH} = 5$, $\chi_i/\chi_{CH} = 2$, and $D_e/\chi_{CH} = 1$. Lower values would imply higher T_e and T_i on axis.

Two TGLF predictions are shown, one with the standard turbulence quench due to E×B sheared flow derived using the input v_ϕ. The other assumes no flow shear. The TGLF predictions for T_e and T_i with quench are close to the predictions shown from the previous PTRANSP run [6]. The TGLF predictions without flow shear (labeled alphae0) are lower. The differences between T_e and T_i with and without flow shear are larger with TGLF than with the old PTRANSP-GLF23 results.

The new PT-SOLVER predictions using GLF23 predictions assuming no flow shear are also close to the TGLF predictions with quench. The new PT-SOLVER GLF23 predictions assuming full strength flow shear (not shown) are considerably higher. This appears to be due mainly to the assumption of low transport in the inner region (inside q=1) causing the ion heat flux to build up.

Density profiles are not predicted by the runs shown in figure 7. Example of density predictions from PTSOLVER with GLF23 are shown in figure 8. The source rate for the electron density is computed from the beam ionization rate and an estimate of the recycling, fueling, and gas puffing rates.

These are small in the modeled region ($x \leq 0.8$). The source rate for the D and T is negative near the axis due to their losses from DT fusion. The electron and combined ion density profiles are compared with the GLF23 results shown in figure 7. A slight peaking of n_e and hollowing of n_i are seen. The T_e profile is 3 % higher and the T_i profile is 5 % higher than the results for the flat profile shown in figure 7.

6. Discussion Verification and validation of TGLF in PTRANSP is being performed. Comparisons with measurements in the small set of plasmas shown here over-predict either T_e or T_i. Temperatures near the magnetic axis where TGLF fluxes vanish depend sensitively on assumptions of the transport, and add ambiguity to the comparisons with measurements.

An exploration of ITER predictions with TGLF in PTRANSP and PT-SOLVER has been done. The low transport near the magnetic axis predicted by TGLF and simple neoclassical models implies large central temperatures. This indicates that improved treatment of transport in the core is needed. Another issue needing further exploration is treatment of rotation and flow shear of turbulence. Another is fast ion turbulence, not included in the predictions. Runs with more ion species are being explored to study issues such as possible differences in the transport of D and T, and transport of impurities including ash needs to be investigated.

Acknowledgments - This manuscript has been authored by Princeton University under Contract Number DE-AC02-09CH11466 with the U.S. Department of Energy. This work was supported in part by the US Department of Energy under DE-FG02-95ER54309 and was supported in part by EURATOM and carried out within the framework of the European Fusion Development Agreement. The views and opinions expressed herein do not necessarily reflect those of the European Commission.

[1] Budny R.V., Nucl. Fusion **49**, (2009) 085008.
[2] Budny R.V., Andre R., Bateman G., Halpern F., Kessel C.E., A. Kritz and D. McCune, Nucl. Fusion **48**, (2008) 075005.
[3] Halpern F.D., Kritz A.H., Bateman . G., Pankin A.Y., Budny R.V., and McCune, D.C., Phys. of Plasmas **15** (2008) 062505.
[4] T. Rafiq, A. H. Kritz, G. Bateman, C. Kessel, D. C. McCune, and R. V. Budny Phys. Plasmas **18**, (2011) 112508.
[5] A.H. Kritz, T. Rafiq, C. Kessel, G. Bateman, D.C. McCune, R.V. Budny and A.Y. Pankin Nucl. Fusion **51**, (2011) 51 123009.
[6] Budny R.V., Nucl. Fusion **52**, (2012) 013001.
[7] Waltz R.E., Staebler G.M., Dorland W., Hammett G.W., Kotschenreuther M., and J. A. Koning, Phys. of Plasmas **4** (1997) 2482.
[8] Kinsey J.E., Staebler G.M., Waltz R.E., Phys. of Plasmas, **9** (2002) 1676.
[9] Staebler G.M., Kinsey J.E. and Waltz R.E. 2007 Phys. Plasmas **14** (2007) 055909
[10] Kinsey J.E., Staebler G.M. and Waltz R.E., Phys. Plasmas **15** (2008) 055908.
[11] Candy J, Waltz R., J. Comput. Phys. **186** 545 (2003).
[12] Kinsey J.E., Staebler G.M., Waltz R., Candy J., Budny R.V., Nuclear Fusion **51** 083001 (2011).
[13] Kinsey J.E., Waltz R., and J. Candy Phys. of Plasmas **14** 102306 (2007).
[14] http:w3.pppl.gov/ntcc
[15] Jardin, S., *et al.* J. Comput. Phys. **227** 8769 (2008).
[16] Pereverzev G.V., and Corrigan, G., Comput. Phys. Com. **179** 579 (2008).
[17] D. McCune, http:w3.pppl.gov/ntcc/PlasmaState/
[18] Nunes I., *et al.*, Proceedings of the 23th IAEA Fusion Energy Conference 2010, (EXE/P8-03).
[19] Budny R.V., Ernst, D.E., *et al.*, Physics of Plasmas, Vol 7 (2000) p 5038-5050.
[20] J.E. Kinsey, G.M. Staebler, and C.C. Petty, Phys. Plasmas **17**, (2010) 122315.
[21] J Hobirk, F Imbeaux, F Crisanti, P Buratti, C D Challis, E Joffrin, B Alper, *et al.,* Plasma Phys. Cont. Fusion, **54** (2012) 095001.

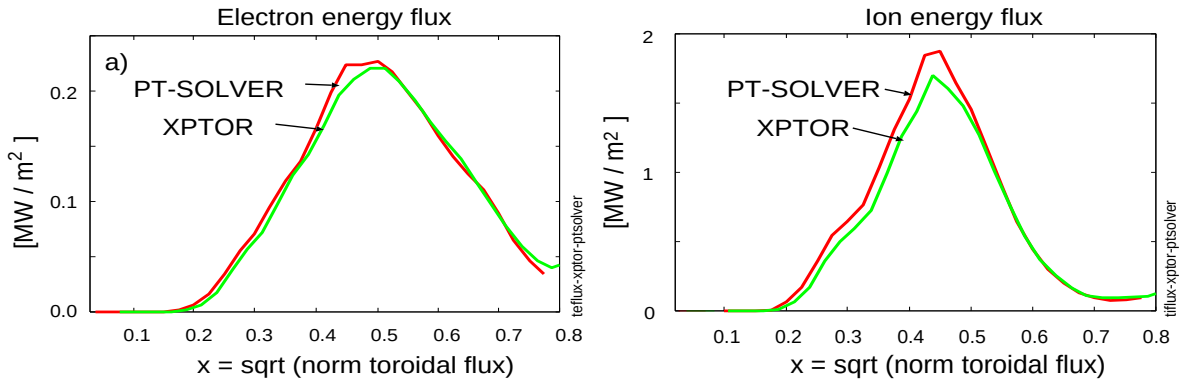

FIG. 1: Comparisons of the electron a) and ion b) initial heat fluxes computed for a DIII-D plasma by XPTOR and PT-SOLVER.

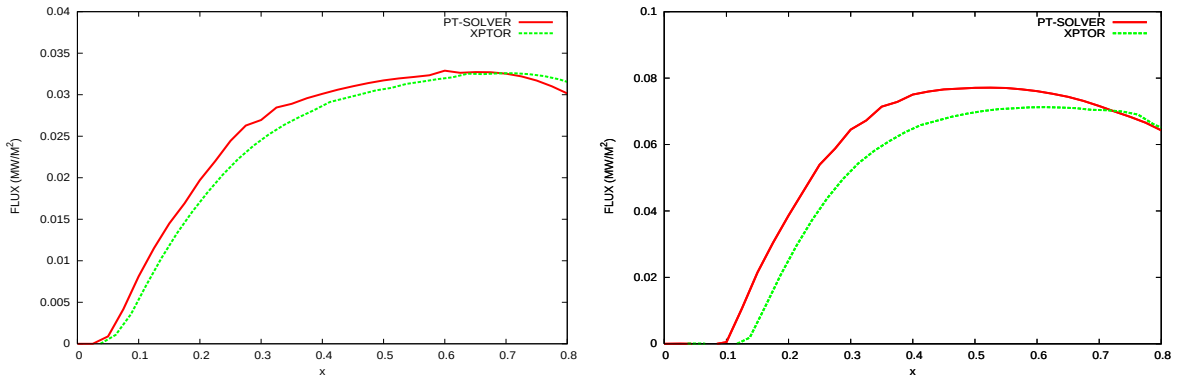

FIG. 2: Comparisons of the electron (left) and ion (right) converged heat fluxes computed by PT-SOLVER and XPTOR for the case shown in figure 1. The predicted T_e and T_i profiles (not shown) are close for both codes.

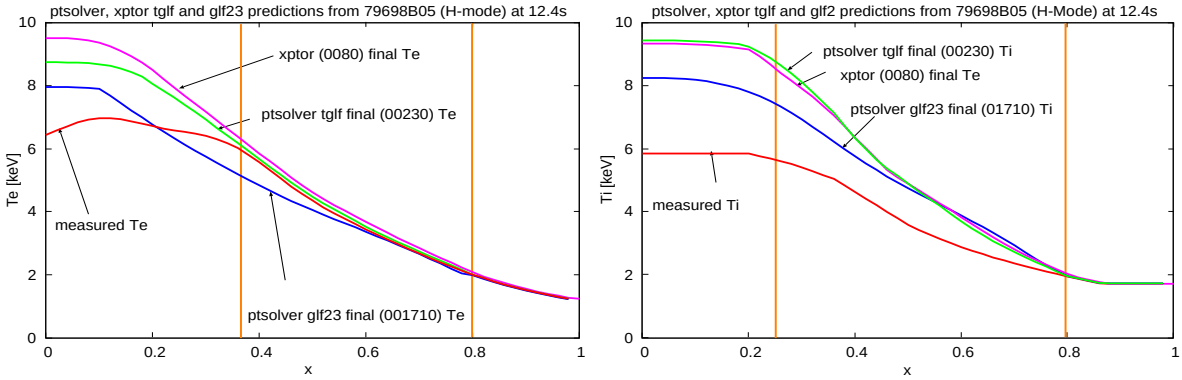

FIG. 3: Comparisons of predicted electron a) and ion b) temperatures computed by PT-SOLVER and XPTOR using TGLF and GLF23. This JET H-mode has I_p=4.5MA and B_0=3.6T [18]. The TGLF electron heat transport is negligible for $x \leq 0.35$, and the TGLF ion heat transport is negligible for $x \leq 0.25$. The numbers in parentheses are the number of PT-SOLVER iterations for convergence.

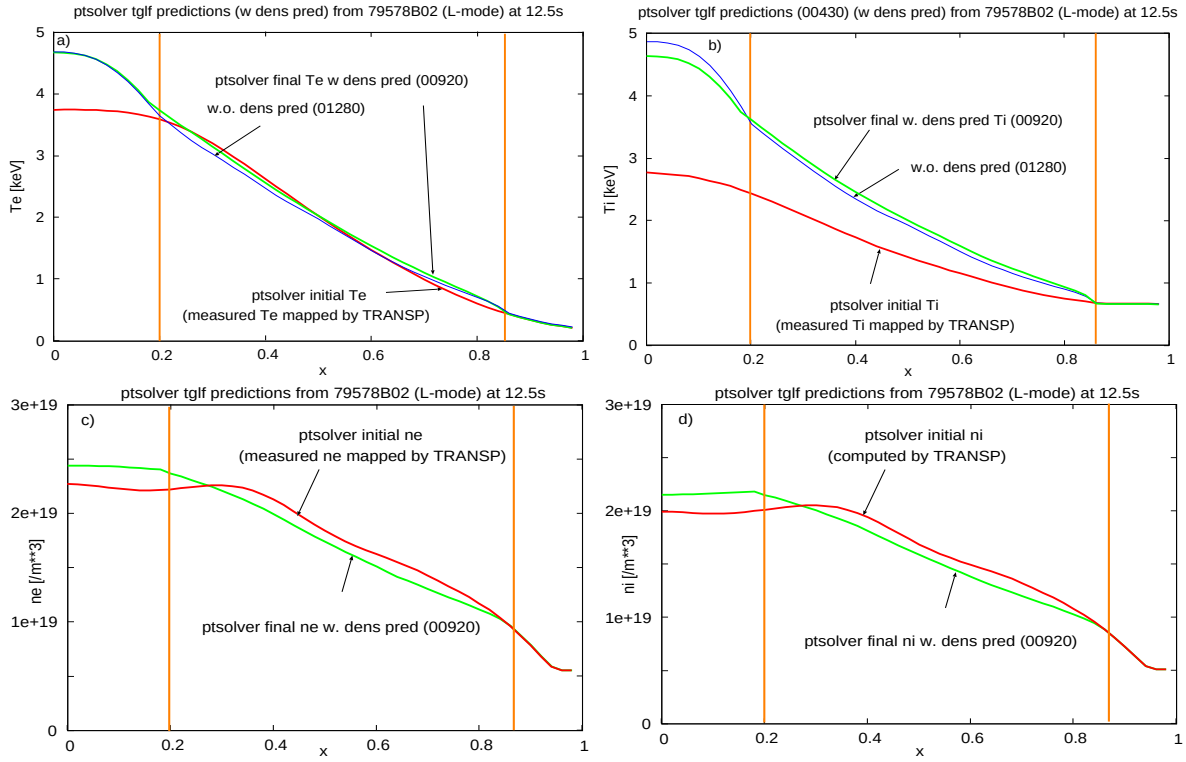

FIG. 4: Comparisons of PT-SOLVER TGLF predicted and TRANSP mapped electron a) and ion b) temperatures and electron c) and average ion d) densities for a JET L-mode. The TGLF transport is near zero for x $\leq$ 0.2.

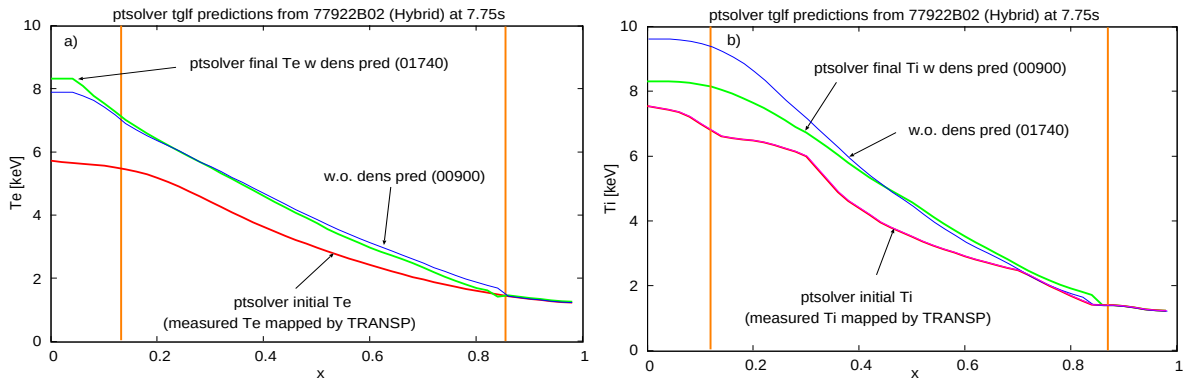

FIG. 5: Comparisons of PT-SOLVER TGLF predicted and TRANSP mapped electron a) and ion b) temperatures for a JET Hybrid. The TGLF transport is near zero for x $\leq$ 0.18.

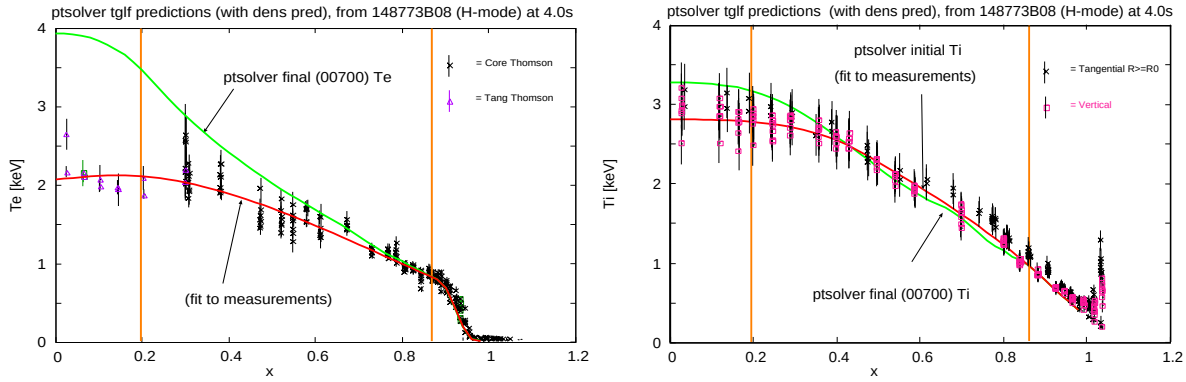

FIG. 6: Comparisons of predicted and measured electron a) and ion b) temperatures for a DIII-D ITER baseline simulation shot. The TGLF transport is near zero for x $\leq$ 0.2. The outer boundary for PT-SOLVER is taken at x=0.84.

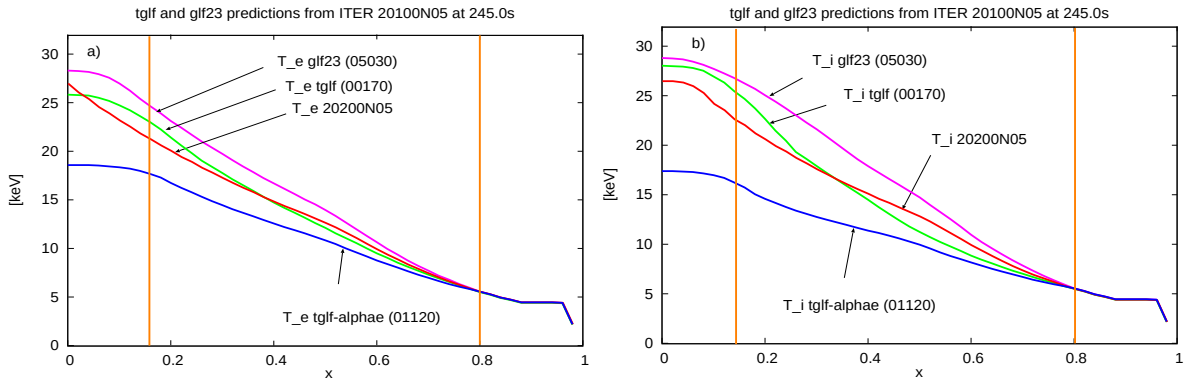

FIG. 7: Comparisons of electron a) and ion b) temperatures for ITER baseline simulation predicted by PT-SOLVER with GLF23 and TGLF and by previous PTRANSP predictions ([6]) using GLF23 in the old solver and achieving $Q_{\rm DT} = 9$ after the heating is lowered to 50 MW. The TGLF transport is near zero for x $\leq$ 0.2. The lowest predictions are from TGLF with no flow shear.

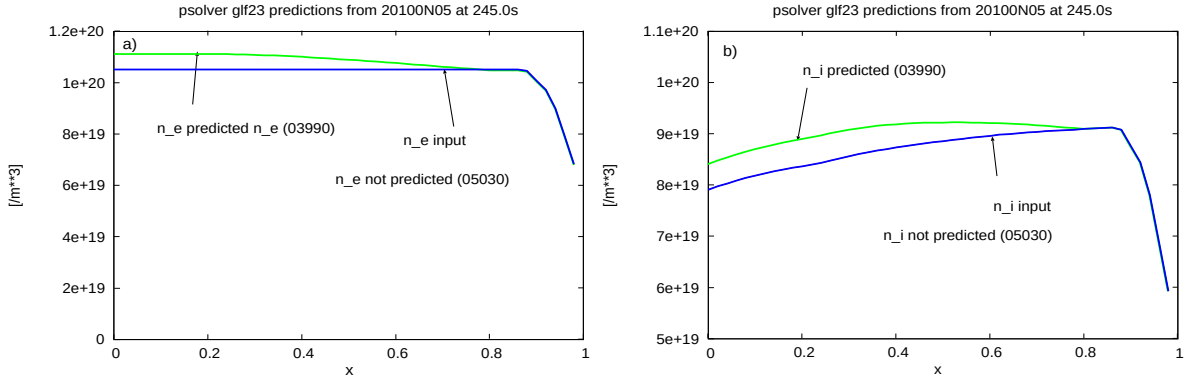

FIG. 8: Predictions of electron a) and ion b) density profiles predicted by PT-SOLVER with GLF23 compared with the GLF23 case in figure 6. The T_e profile is 3 % higher and the T_i profile is 5 % higher than the results shown in figure 7.

The Princeton Plasma Physics Laboratory is operated
by Princeton University under contract
with the U.S. Department of Energy.

Information Services
Princeton Plasma Physics Laboratory
P.O. Box 451
Princeton, NJ 08543

Phone: 609-243-2245
Fax: 609-243-2751
e-mail: pppl_info@pppl.gov
Internet Address: http://www.pppl.gov